

Supporting Information

Accelerating Crystallization of Open Organic Materials by Poly(ionic liquid)s

Su-Yun Zhang⁺, Han Miao⁺, He-min Zhang⁺, Jun-Hao Zhou, Qiang Zhuang, Yu-Jia Zeng, Zhiming Gao, Jiayin Yuan,^{} and Jian-Ke Sun^{*}*

anie_202008415_sm_miscellaneous_information.pdf

Experimental Procedures

1. Chemicals and Instrumentation

All chemicals were from commercial sources and used without further purification.

Transmission electron microscopy (TEM) was performed on a JEOL 2010FS transmission electron microscope operated at 120 kV. Powder X-ray diffraction (PXRD) was carried out on an X-ray diffractometer of Rigaku, Ultima IV. X-ray photoelectron spectroscopy (XPS) studies were performed on a ThermoFisher ESCALAB250 X-ray photoelectron spectrometer (powered at 150 W) using Al K α radiation ($\lambda = 8.357 \text{ \AA}$). To compensate for surface charging effects, all XPS spectra were referenced to the C 1s neutral carbon peak at 284.6 eV. ^1H nuclear magnetic resonance ($^1\text{H-NMR}$) measurements were carried out at room temperature on a Bruker DPX-400 spectrometer in different deuterated solvents. The N $_2$ sorption isotherms were measured on automatic volumetric adsorption equipment (Belsorp-mini II).

2. Experimental Section

2.1 Synthesis of poly(ionic liquids)

The preparation methods of 4-hexyl-1-vinyl-1,2,4-triazolium iodide and poly(4-hexyl-1-vinyl-1,2,4-triazolium iodide) (denoted as "Ptriaz") were described in the literature (J. K. Sun, Z. Kochovski, W. Y. Zhang, H. Kirmse, Y. Lu, M. Antonietti, J. Yuan, *J. Am. Chem. Soc.*, 2017, 139, 8971–8976.).

The preparation methods of 4-octyl-1-vinyl-1,2,4-triazolium iodide and poly(4-octyl-1-vinyl-1,2,4-triazolium iodide) were described as follows:

Synthesis of 4-octyl-1-vinyl-1,2,4-triazolium iodide: A mixture of 1-vinyl-1,2,4-triazole 1 (5 mL, 5.5g, 57.83 mmol) and a 1.2 equivalent amount of 1-iodooctane were added into a 100 mL round flask, accompanied with 2,6-di-tert-butyl-4-methylphenol (50 mg, 0.227 mol) as the stabilizer. After heated at 50 °C overnight, crude products were precipitated in diethyl ether and washed with the same solvent for three times. Pale yellow powders were obtained after purification.

Synthesis of poly(4-octyl-1-vinyl-1,2,4-triazolium iodide): A mixture of 4-octyl-1-vinyl-1,2,4-triazolium iodide monomer with AIBN (1.5 mol%) as initiator was added to anhydrous DMF (concentration: ~1 g monomer in 10 mL solvent) inside a 100 mL round-bottom schlenk flask. The flask was treated with three freeze-pump-thaw cycles and finally purged with argon. The reaction was stirred at 70 °C for 24 h under argon atmosphere. Yellow powders were obtained after dialysis against water and a vacuum drying process.

The preparation methods of 4-cyanomethyl-1-vinyl-1,2,4-triazolium bis(trifluoromethane sulfonyl)imide and poly(4-cyanomethyl-1-vinyl-1,2,4-triazolium bis(trifluoromethane sulfonyl)imide) were described in the literature (J. K. Sun, W. Zhang, R. Guterman, H. J. Lin, J. Yuan, *Nat. Commun.*, 2018, 9, 1717).

SUPPORTING INFORMATION

The preparation methods of 4-hexyl-1-vinyl-imidazolium iodide and poly(4-hexyl-1-vinyl-imidazolium iodide) (simplified as "PIL-imidaz") were described in the literature (J. C. Salamone, S. C. Israel, P. Taylor, B. Snider, *Polymer*, 1973, 14, 639-644.)

The preparation of poly(1-hexyl-4-vinyl-pyridinium iodide) (denoted as "PIL-py") is as follows: A mixture of commercially purchased poly(4-vinylpyridine) (3 g, $M_w = 1.6 \times 10^5$ g/mol) and a 1.5 equivalent amount of 1-iodohexane in 50 mL of DMF was added into a 150 mL round flask. After heating at 80 °C for 10 h, dark brown powders were obtained upon precipitation in THF, then it was washed with the same solvent for three times. The chemical structure was confirmed by ^1H NMR spectrum in Figure S26.

2.2 Synthesis of open organics

Synthesis of CC3R with Ptri az additive: For the typical synthesis of CC3R, 0.35 mL of chloroform solution containing 1,3,5-triformylbenzene (8 mg, 0.05 mmol) and Ptri az (25 mg, 0.08 mmol) was added by a chloroform solution (0.35 mL) of (R,R)-1,2-diaminocyclohexane (8 mg, 0.07 mmol). The vessel of the mixture solution was capped and left to stand for a certain time to give out the single crystals. The precipitate crystals were collected and dried under vacuum at 80 °C for 24 h.

Synthesis of CC3R without Ptri az additive: The synthetic procedure used above to prepare CC3R-Ptri az was followed without Ptri az additive.

Synthesis of CC3R with PIL-imidaz additive: The synthetic procedure used above to prepare CC3R-Ptri az was followed by using PIL-imidaz containing chloroform instead of Ptri az.

Synthesis of CC3R with PIL-py additive: The synthetic procedure used above to prepare CC3R-Ptri az was followed by using PIL-py containing chloroform instead of Ptri az.

Synthesis of CC3R with triaz monomer additive: The synthetic procedure used above to prepare CC3R-Ptri az was followed by using triaz monomer containing chloroform instead of Ptri az.

Synthesis of BTA-PED COF with poly(4-cyanomethyl-1-vinyl-1,2,4-triazolium bis(trifluoromethane sulfonyl)imide) additive: For the typical synthesis of BTA-PED COF, 0.4 mL of dioxane solution containing 1,3,5-triformylbenzene (10 mg, 0.06 mmol) and 1,4-phenylenediamine (PED) (10 mg, 0.09 mmol), and then 0.4 mL of dmsol solution containing poly(4-cyanomethyl-1-vinyl-1,2,4-triazolium bis(trifluoromethane sulfonyl)imide) (30 mg, 0.07 mmol) was added. The vessel of the mixture solution was capped and left to stand for a certain time to give out the BTA-PED COF precipitate. The precipitate crystals were collected by centrifugation and dried under vacuum at 80 °C for 24 h.

Synthesis of BTA-PED COF without poly(4-cyanomethyl-1-vinyl-1,2,4-triazolium bis(trifluoromethane sulfonyl)imide) additive: The synthetic procedure used above to prepare BTA-PED COF without any additive.

Synthesis of TPA-DACH macrocycle with poly(4-octyl-1-vinyl-1,2,4-triazolium iodide) additive: For the typical synthesis of TPA-DACH macrocycle, 0.3 mL of chloroform solution containing terephthalaldehyde (TPA) (13.4 mg, 0.1 mmol) and poly(4-octyl-1-vinyl-1,2,4-triazolium iodide) (25 mg,

SUPPORTING INFORMATION

0.08 mmol) was added by a chloroform solution (0.3 mL) of (R,R)-1,2-diaminocyclohexane (11.4 mg, 0.1 mmol). The vessel of the mixture solution was capped and left to stand for a certain time to give out the single crystals. The precipitate crystals were collected by centrifugation and dried under vacuum at 80 °C for 24 h.

Synthesis of TPA-DACH macrocycle without poly(4-octyl-1-vinyl-1,2,4-triazolium iodide) additive: The synthetic procedure used above to prepare TPA-DACH macrocycle without any additive.

Synthesis of IPA-DACH macrocycle with P For the typical synthesis of IPA-DACH macrocycle, 0.3 mL of chloroform solution containing isophthalaldehyde (IPA) (13.4 mg, 0.1 mmol) and P

Synthesis of IPA-DACH macrocycle without P The synthetic procedure used above to prepare IPA-DACH macrocycle without any additive.

2.3 Synthesis of catalyst for AB methanolysis reaction

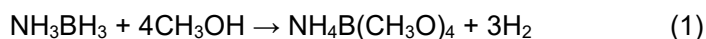
Synthesis of Rh/CC3R-P In a typical synthesis, 4 mL of methanol containing 5 mg of CC3R (with P3 (0.01 mol Rh in content). The resultant mixture solution was further homogenized after aging for 20 min. Then, 0.5 mL of methanol solution containing 5 mg of NaBH₄ was immediately added into the above solution with vigorous shaking, resulting in a well dispersion of Rh/CC3R-P

Synthesis of Rh/CC3R catalyst. The synthetic procedure used above to prepare Rh/CC3R-P

Synthesis of Rh-SP-Free catalyst. The synthetic procedure used above to prepare Rh/CC3R-P

2.4 Catalytic activity characterization

Procedure for the methanolysis of AB by Rh/CC3R-P The reaction apparatus for measuring the hydrogen evolution from the methanolysis of AB is as follows. In general, the as-synthesized Rh/CC3R-P



SUPPORTING INFORMATION

Procedures for the methanolysis of AB by Rh-CC3R catalyst and Rh-SP-Free catalysts: The procedures for the methanolysis of AB were similar to that of Rh/CC3R-Ptriaz catalyst except different catalysts were used.

3. Results and Discussion

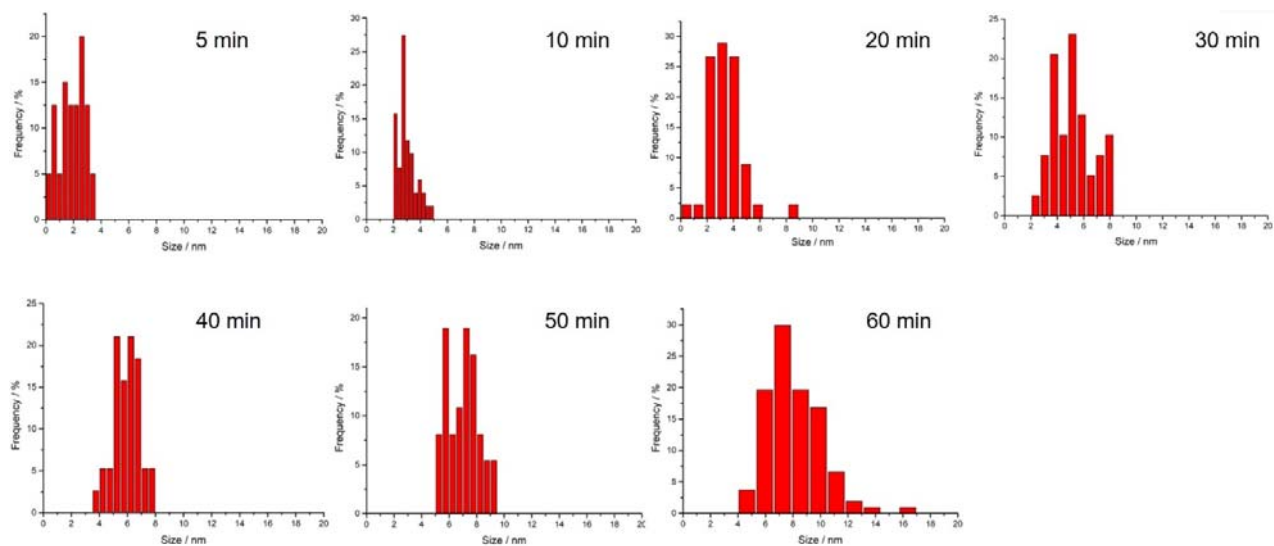


Figure S1. Time dependent size-distribution of CC3R Crystals in the presence of Ptriaz.

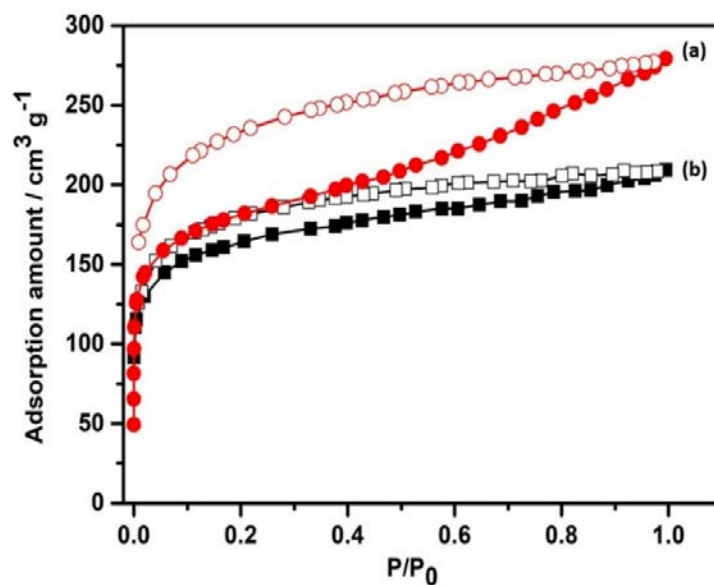


Figure S2. The N_2 sorption isotherms of (a) CC3R-Ptriaz and (b) CC3R (without acid catalyst) at 77 K. Filled and open symbols represent adsorption and desorption branches, respectively.

SUPPORTING INFORMATION

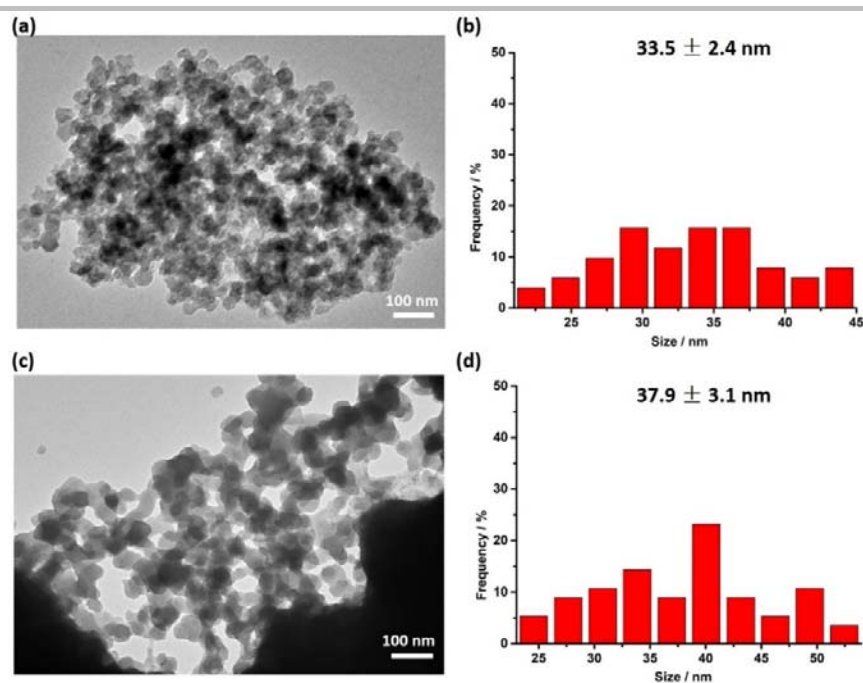


Figure S3. Images of crystallites and corresponding size distributions of BTA-PED COF with (a,b) and without (c,d) poly(4-cyanomethyl-1-vinyl-1,2,4-triazolium bis(trifluoromethane sulfonyl)imide) after reaction for 5 and 300 min, respectively.

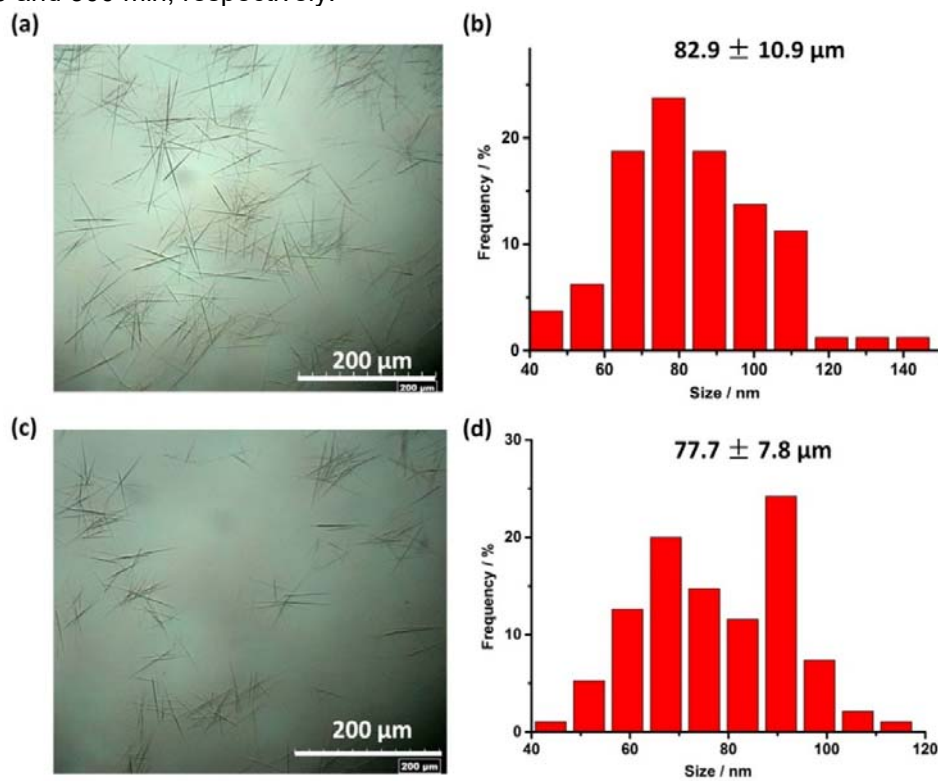


Figure S4. Images of crystals and corresponding size distributions of TPA-DACH macrocycle single crystals with (a,b) and without (c,d) poly(4-octyl-1-vinyl-1,2,4-triazolium iodide) after reaction for 30 and 300 min, respectively.

SUPPORTING INFORMATION

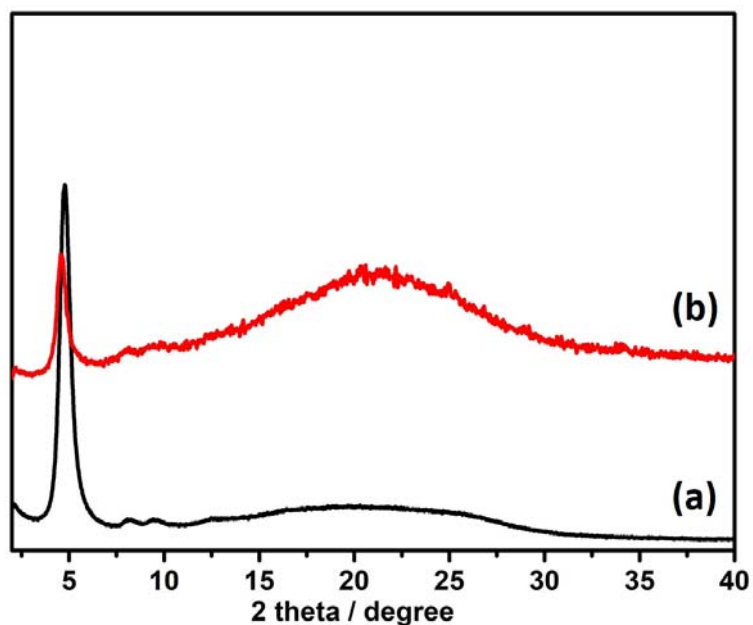


Figure S5. PXRD patterns of (a) BTA-PED COF from literature method (*Chem. Lett.* 2015, 44, 1488–1490), (b) as-synthesized one in the presence of PIL additive.

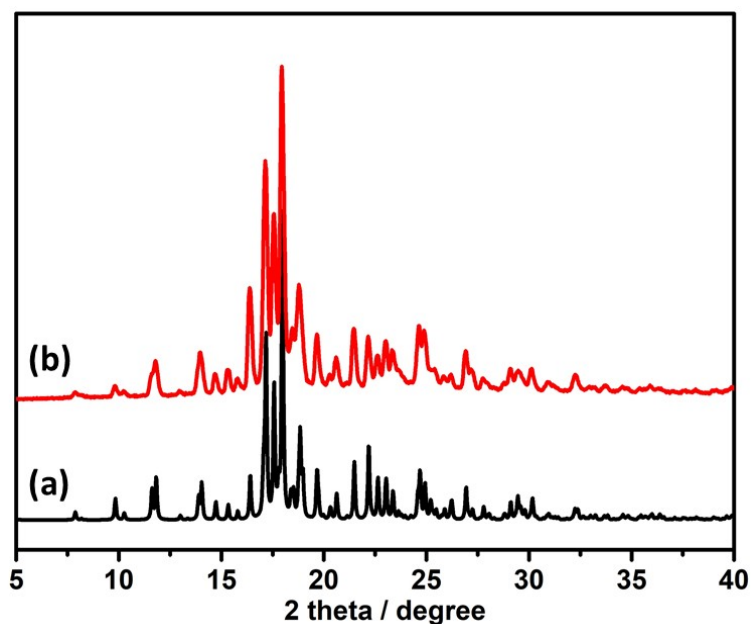


Figure S6. PXRD patterns of (a) simulated TPA-DACH macrocycle single crystal re-crystallized from ethyl acetate from literature (*J. Org. Chem.* 2000, 65, 5768–5773), (b) as-synthesized one in the presence of PIL additive, which was further re-crystallized from ethyl acetate.

SUPPORTING INFORMATION

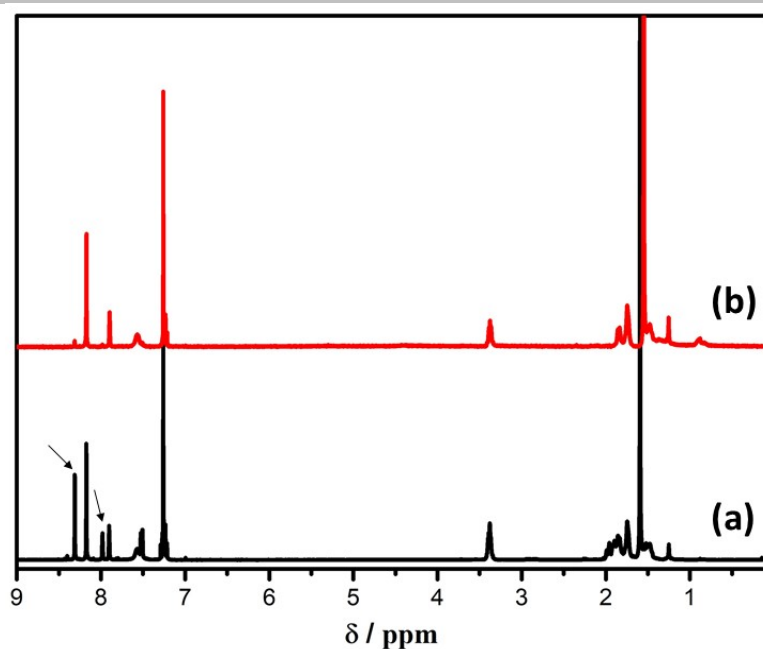


Figure S7. The ^1H NMR spectra of IPA-DACH macrocycle crystals synthesized in PIL-free condition without further purification (a), the [2+2] cyclocondensation byproduct with signal at 8.3 and 7.9 ppm (*Chem. Commun.* 2010, 46, 4315-4317) could be detected with estimated amount of $\sim 45\%$ in the final crystals, while such thermodynamic byproduct could be effectively suppressed in the presence of PIL catalyst (less than 4 %) and without further purification (b).

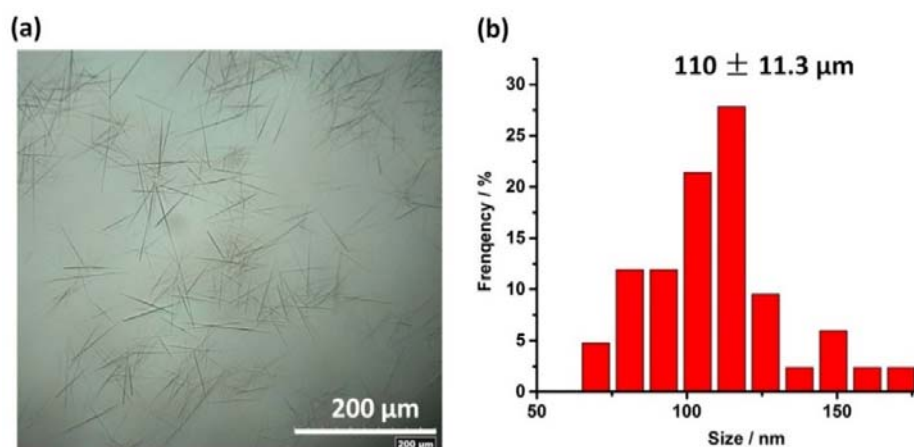


Figure S8. Optical microscopy images of crystals (a) and corresponding size distributions (b) of IPA-DACH macrocycle obtained in the presence of PIL.

SUPPORTING INFORMATION

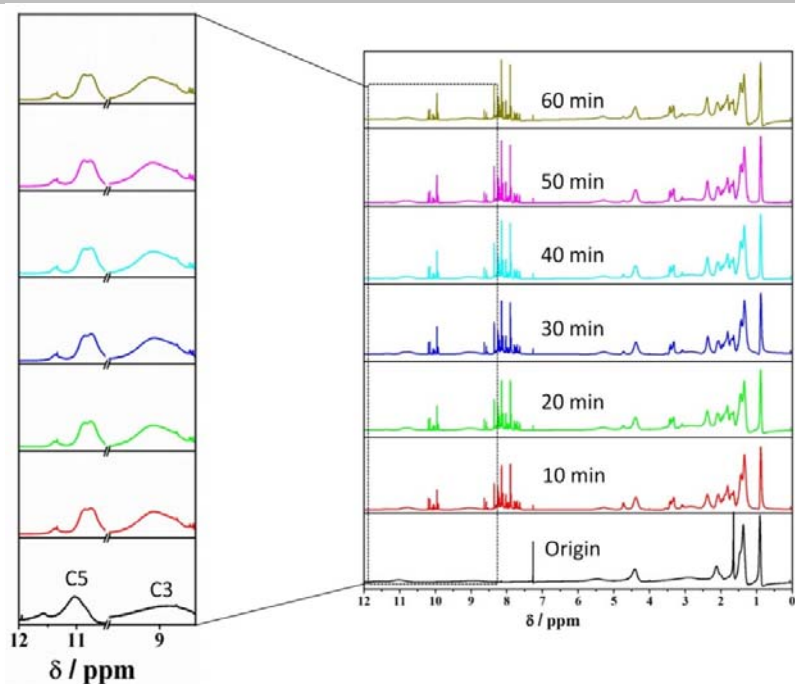


Figure S9. In situ ^1H NMR spectra of the CC3R synthesis mixtures in P triaz in deuterated chloroform at room temperature. The corresponding C5- and C3-protons in P triaz during the CC3R synthesis with higher magnification was highlighted in left column.

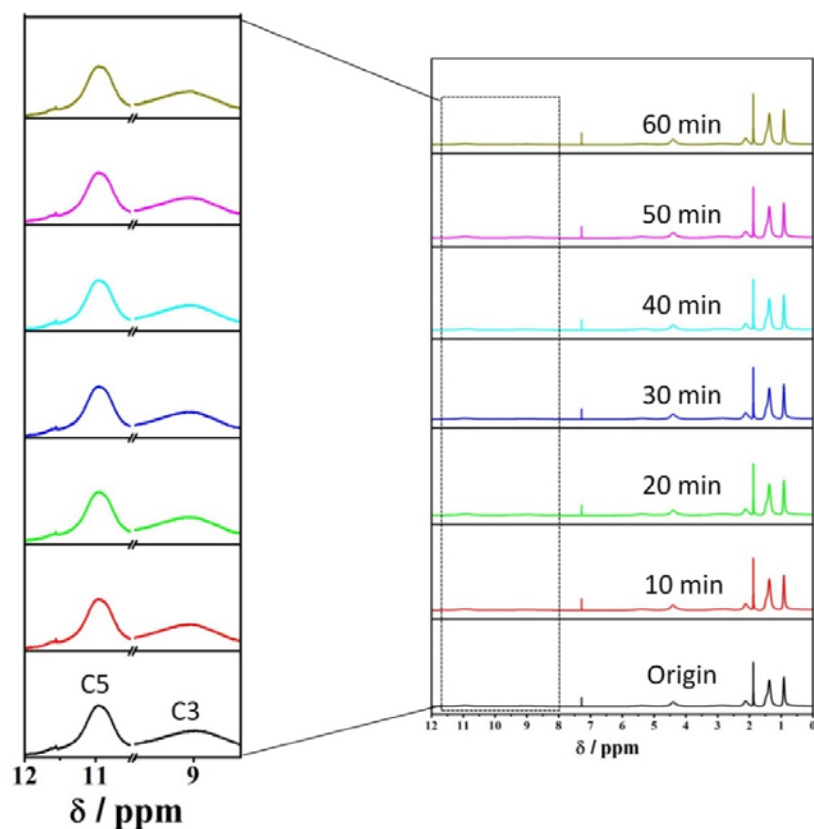


Figure S10. In situ ^1H NMR spectra of pure P triaz in deuterated chloroform at room temperature. The corresponding C5- and C3-protons in P triaz with higher magnification was highlighted in left column.

SUPPORTING INFORMATION

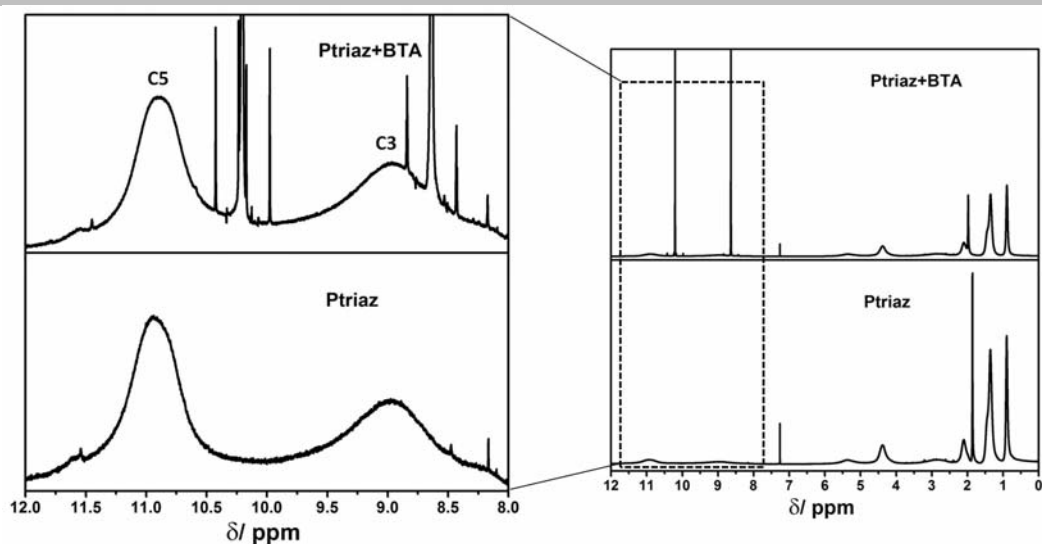


Figure S11. In situ ^1H NMR spectra of pure Ptriaz and Ptriaz-BTA mixture in deuterated chloroform at room temperature. The corresponding C5- and C3-protons with higher magnification was highlighted in left column.

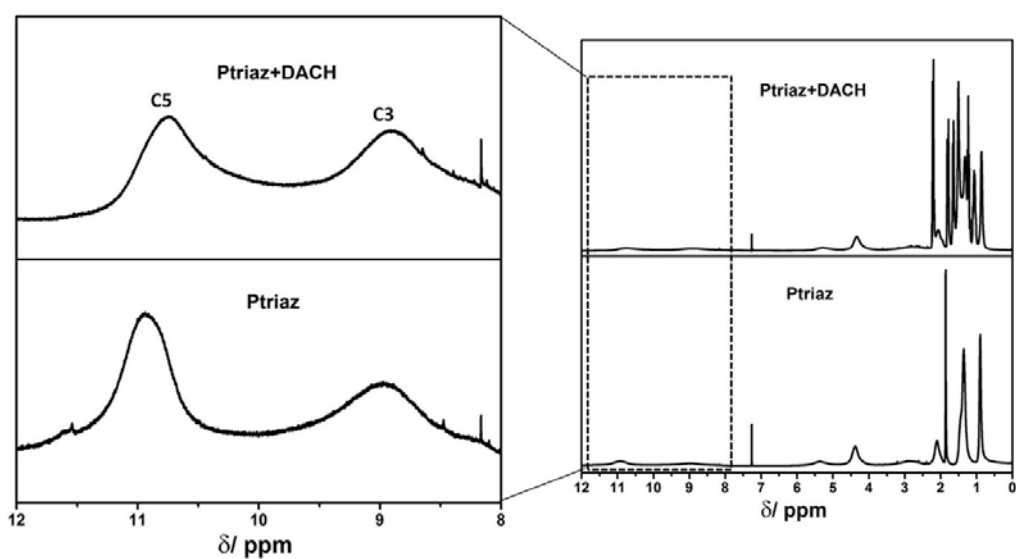


Figure S12. In situ ^1H NMR spectra of pure Ptriaz and Ptriaz-DACH mixture in deuterated chloroform at room temperature. The corresponding C5- and C3-protons with higher magnification was highlighted in left column.

SUPPORTING INFORMATION

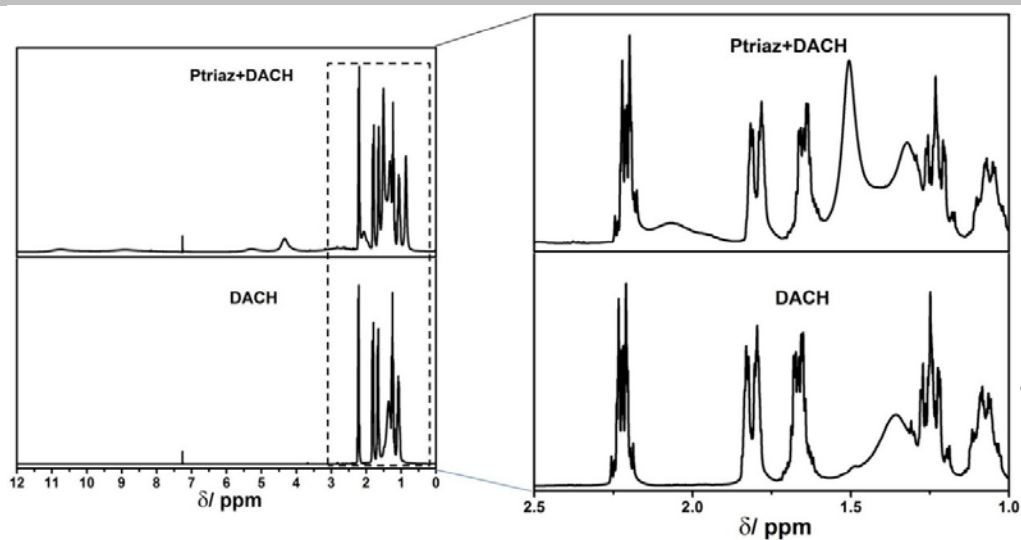


Figure S13. In situ ^1H NMR spectra of pure DACH and Ptriaz-DACH mixture in deuterated chloroform at room temperature. The higher magnification was highlighted in right column.

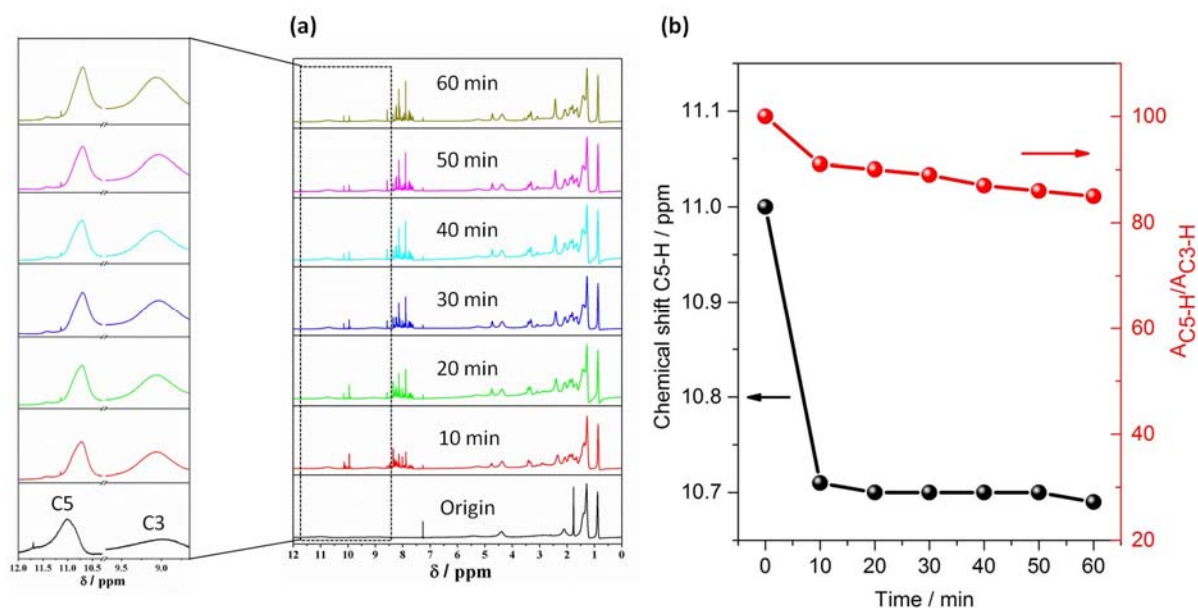


Figure S14. a, In situ ^1H NMR spectra of the CC3R synthesis mixtures in poly(4-octyl-1-vinyl-1,2,4-triazolium iodide) in deuterated chloroform at room temperature. The corresponding C5- and C3-protons in poly(4-octyl-1-vinyl-1,2,4-triazolium iodide) during the CC3R synthesis with higher magnification was highlighted in left column. b, Chemical shift (dark line) and integration of C5- proton peaks (red line) in poly(4-octyl-1-vinyl-1,2,4-triazolium iodide) against time.

SUPPORTING INFORMATION

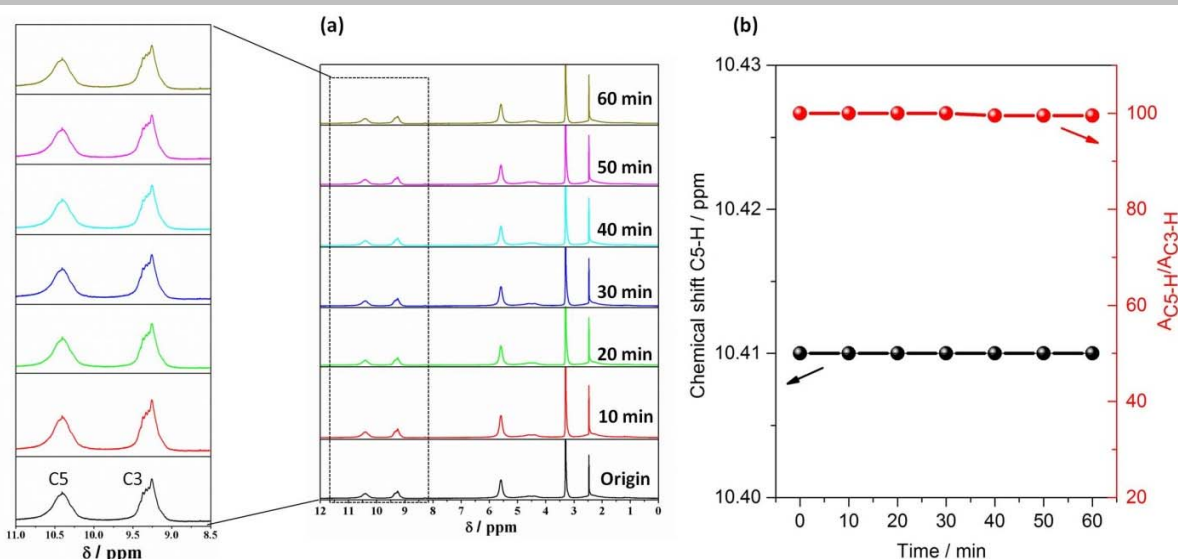


Figure S15. a, In situ ^1H NMR spectra of pure poly(4-cyanomethyl-1-vinyl-1,2,4-triazolium bis(trifluoromethane sulfonyl)imide) in deuterated DMSO at room temperature. The corresponding C5- and C3-protons in poly(4-cyanomethyl-1-vinyl-1,2,4-triazolium bis(trifluoromethane sulfonyl)imide) with higher magnification was highlighted in left column. b, Chemical shift (dark line) and integration of C5-proton peaks (red line) in poly(4-cyanomethyl-1-vinyl-1,2,4-triazolium bis(trifluoromethane sulfonyl)imide) against time.

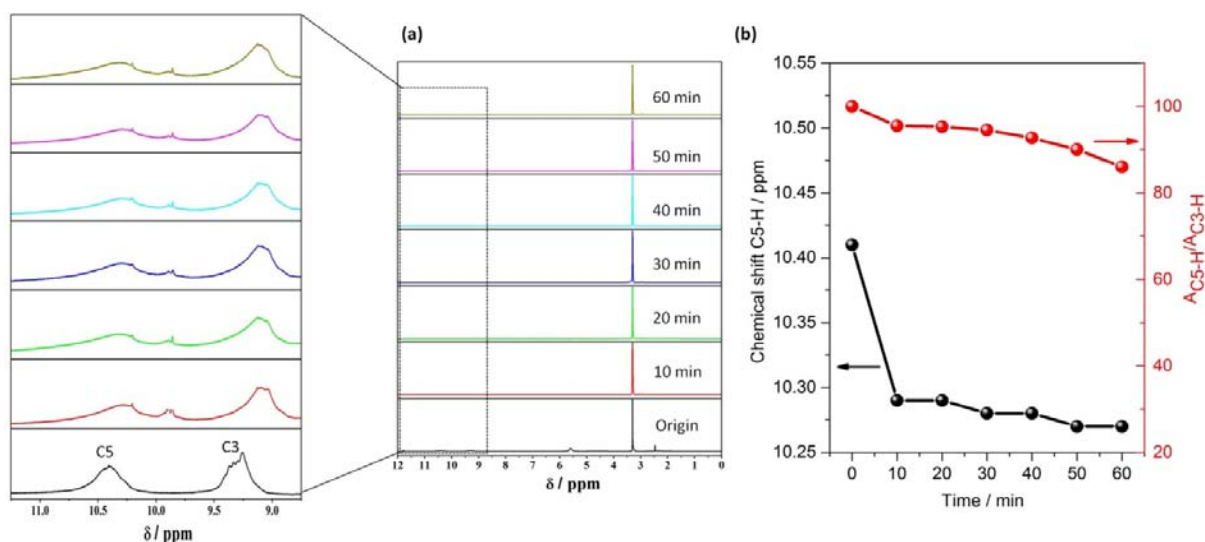


Figure S16. a, In situ ^1H NMR spectra of the BTA-PED COF synthesis mixtures in poly(4-cyanomethyl-1-vinyl-1,2,4-triazolium bis(trifluoromethane sulfonyl)imide) in deuterated DMSO at room temperature. The corresponding C5- and C3-protons in poly(4-cyanomethyl-1-vinyl-1,2,4-triazolium bis(trifluoromethane sulfonyl)imide) during the BTA-PED COF synthesis with higher magnification was highlighted in left column. b, Chemical shift (dark line) and integration of C5-proton peaks (red line) in poly(4-cyanomethyl-1-vinyl-1,2,4-triazolium bis(trifluoromethane sulfonyl)imide) against time.

SUPPORTING INFORMATION

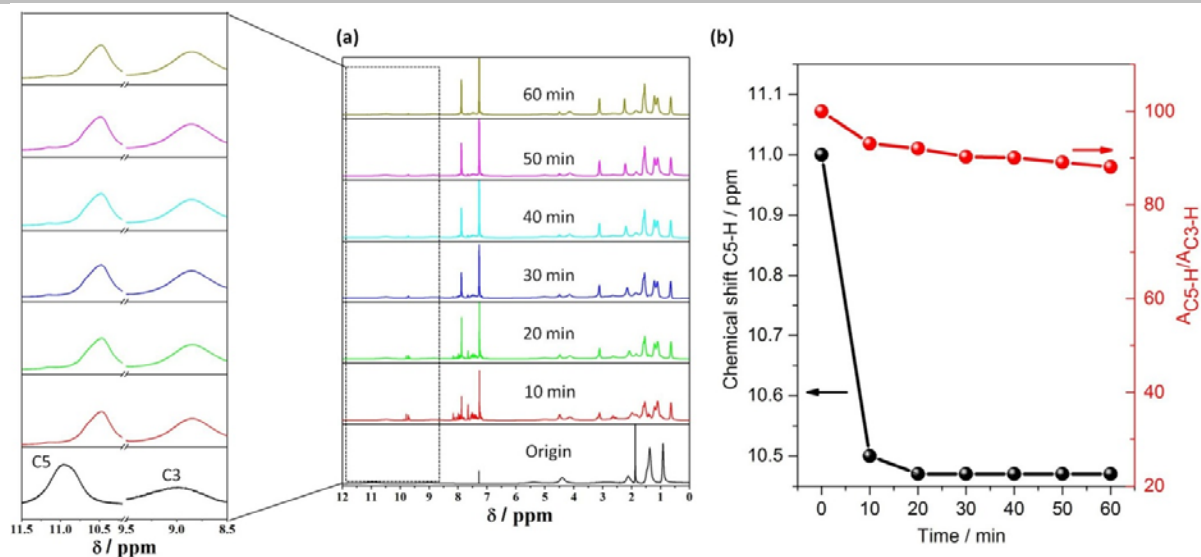


Figure S17. a, In situ ^1H NMR spectra of the TPA-DACH macrocycle synthesis mixtures in poly(4-octyl-1-vinyl-1,2,4-triazolium iodide) in deuterated chloroform at room temperature. The corresponding C5- and C3-protons in poly(4-octyl-1-vinyl-1,2,4-triazolium iodide) during the TPA-DACH macrocycle synthesis with higher magnification was highlighted in left column. b, Chemical shift (dark line) and integration of C5- proton peaks (red line) in poly(4-octyl-1-vinyl-1,2,4-triazolium iodide) against time.

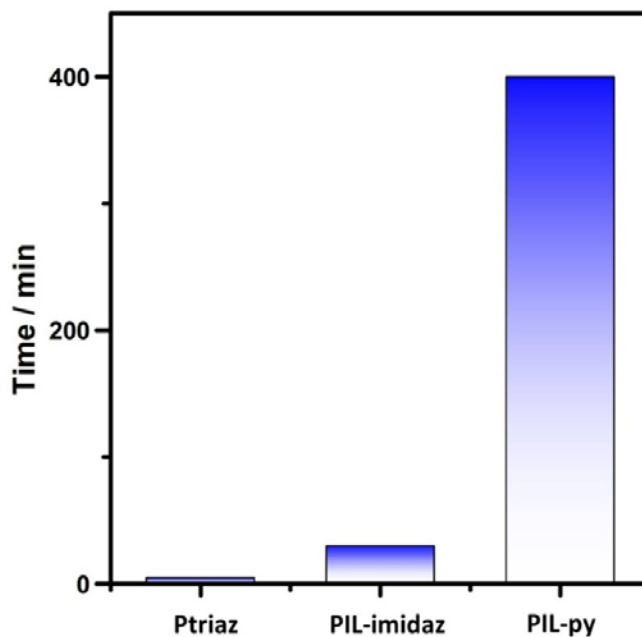


Figure S18. Comparison of the crystallization rate in the presence of the Pptriaz, PIL-imidaz, PIL-py.

SUPPORTING INFORMATION

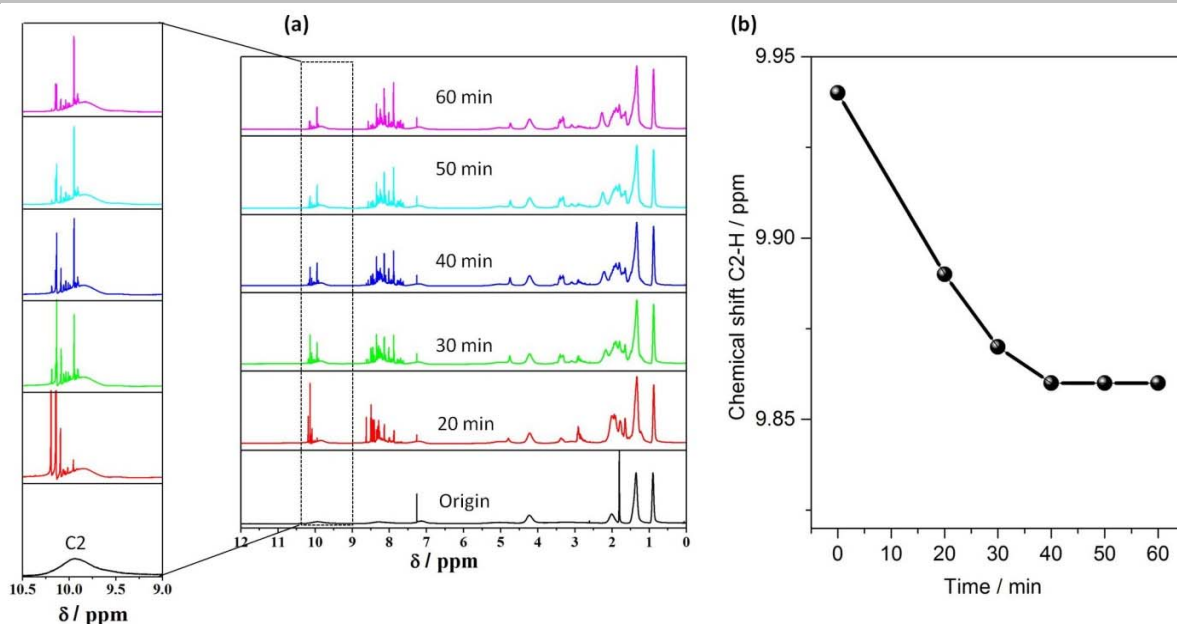


Figure S19. a, In situ ^1H NMR spectra of the CC3R synthesis mixtures in PIL-imidaz in deuterated chloroform at room temperature. The corresponding C2-proton in PIL-imidaz during the CC3R synthesis with higher magnification was highlighted in left column. b, Chemical shift (dark line) of C2- proton peaks in PIL-imidaz against time (The degree of chemical shift is much less than of C5-proton in P triaz). The integration of C2-proton is skipped due to overlap with precursors of CC3R.

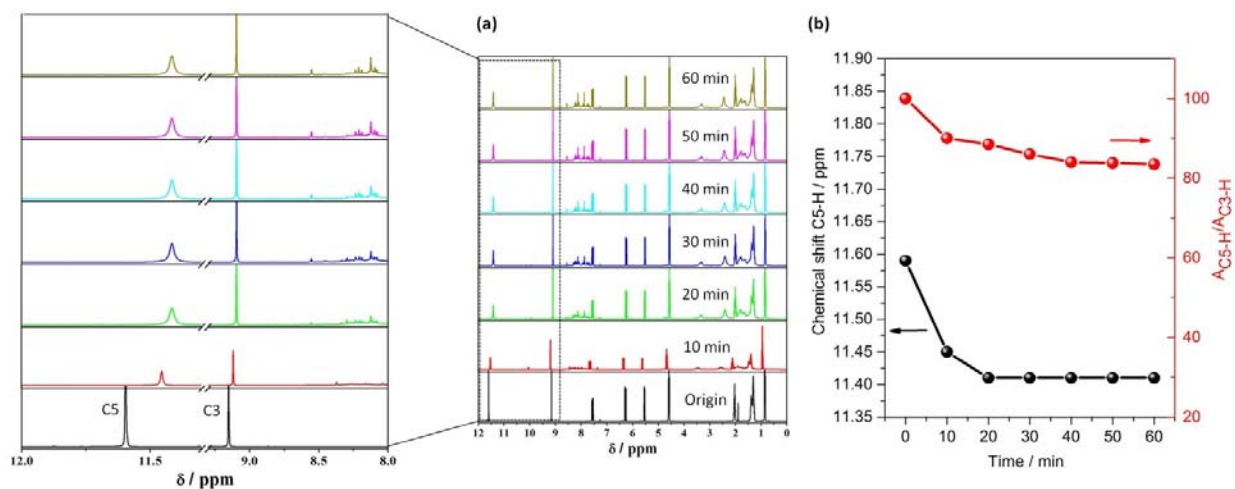


Figure S20. a, In situ ^1H NMR spectra of the CC3R synthesis mixtures in triaz monomer in deuterated chloroform at room temperature. The corresponding C5- and C3-protons in triaz monomer during the CC3R synthesis with higher magnification was highlighted in left column. b, Chemical shift (dark line) and integration of C5- proton peaks (red line) in triaz against time.

SUPPORTING INFORMATION

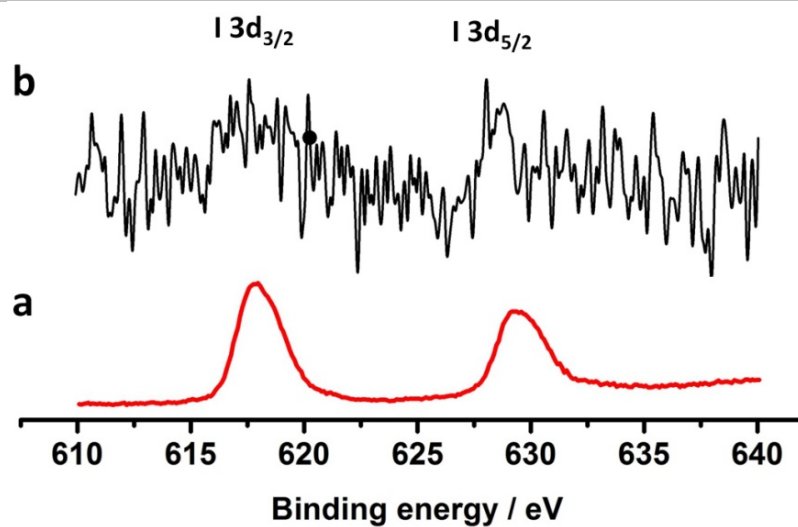


Figure S21. The XPS spectra for I 3d signals of P triaz (a) and CC3R-P triaz (b).

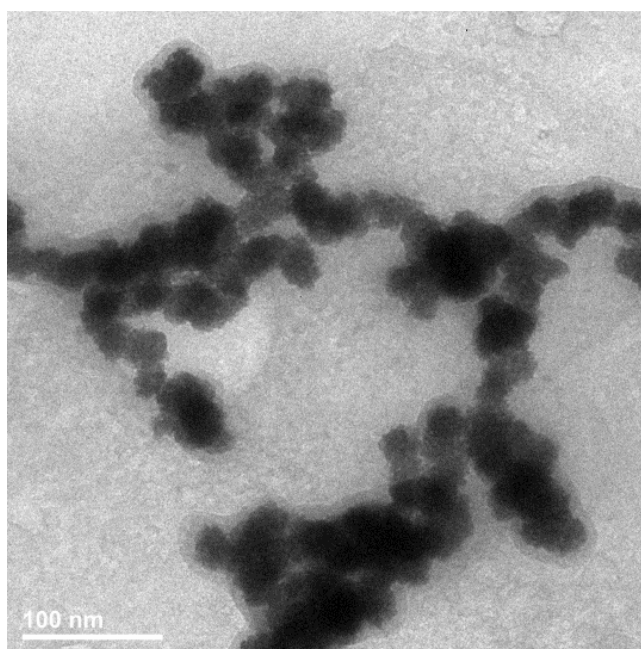


Figure S22. The bright field (BF) TEM image of Rh-SP-Free catalyst.

SUPPORTING INFORMATION

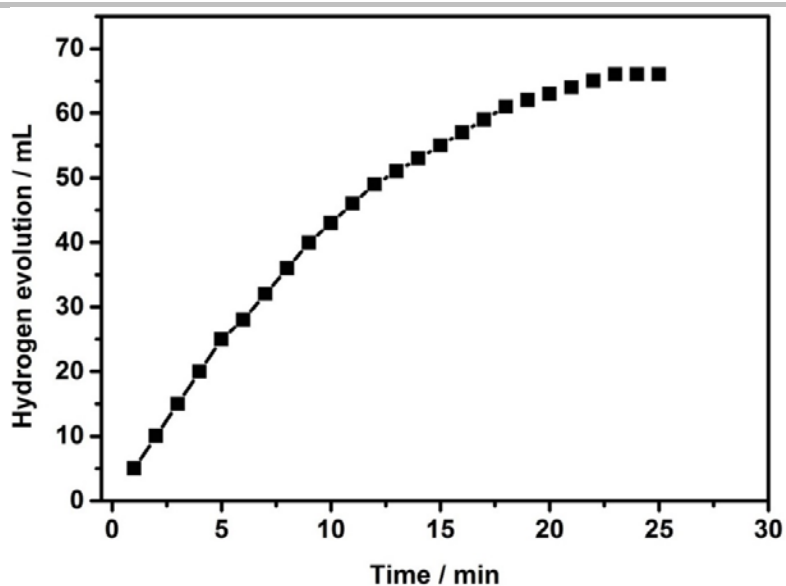


Figure S23. Time course plots of H₂ generation for the methanolysis of ammonia borane (AB) over the Rh-SP-Free catalyst at 298 K (Rh/AB = 0.01).

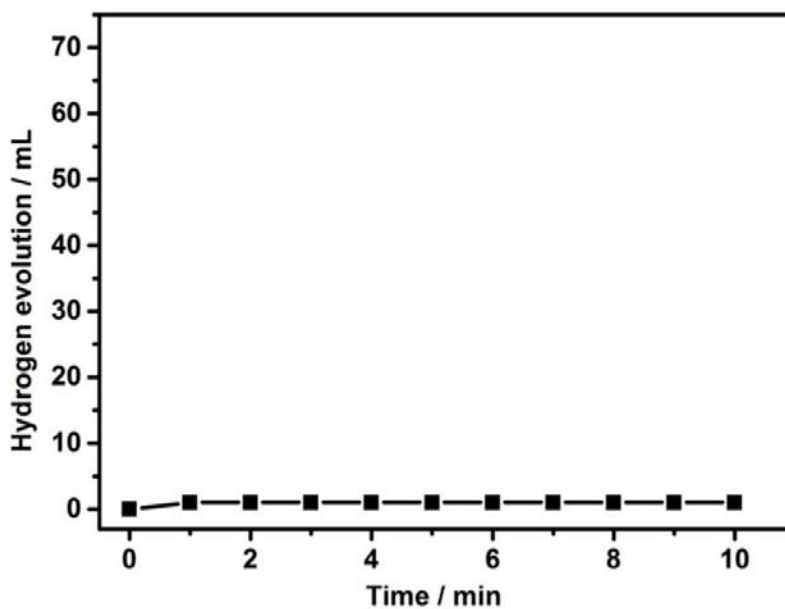


Figure S24. Time course plots of H₂ generation for the methanolysis of AB over the Ptriag at 298 K.

SUPPORTING INFORMATION

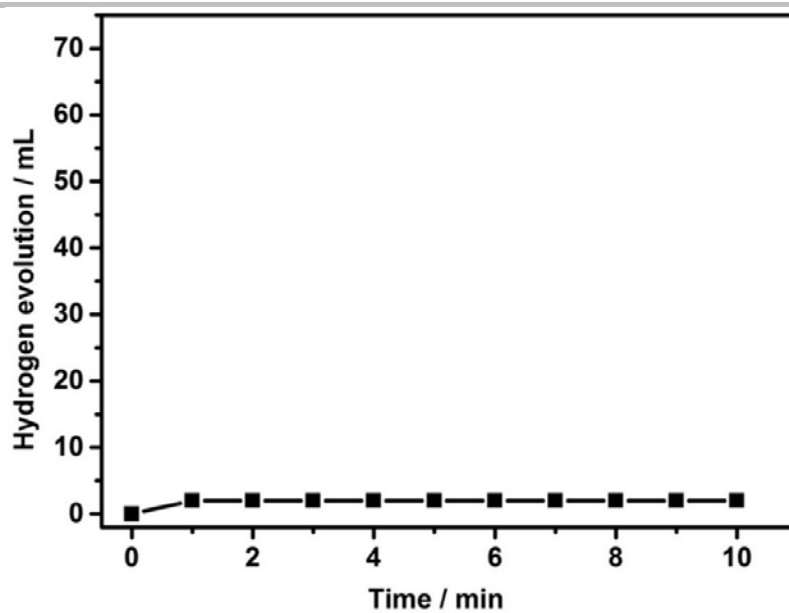


Figure S25. Time course plots of H₂ generation for the methanolsis of AB over the CC3R at 298 K.

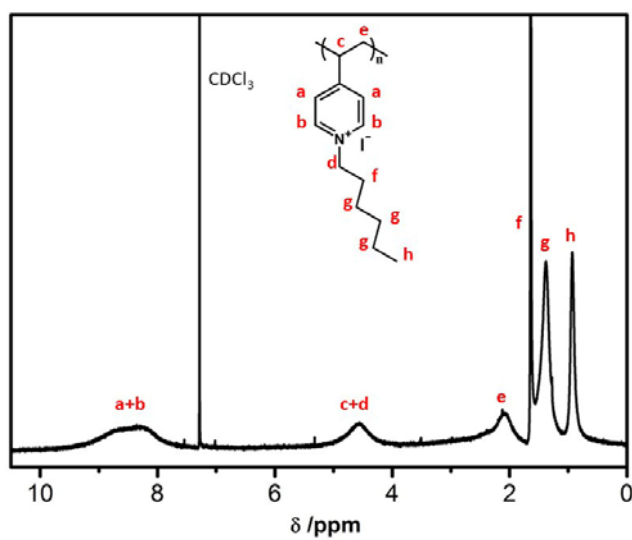


Figure S26. Chemical structure and ¹H-NMR spectrum of PIL-py.

SUPPORTING INFORMATION

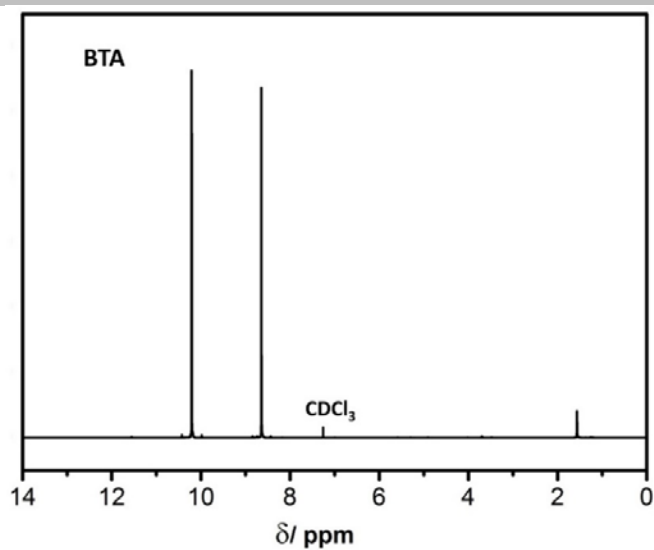


Figure S27. The ¹H-NMR spectrum of BTA in CDCl₃.

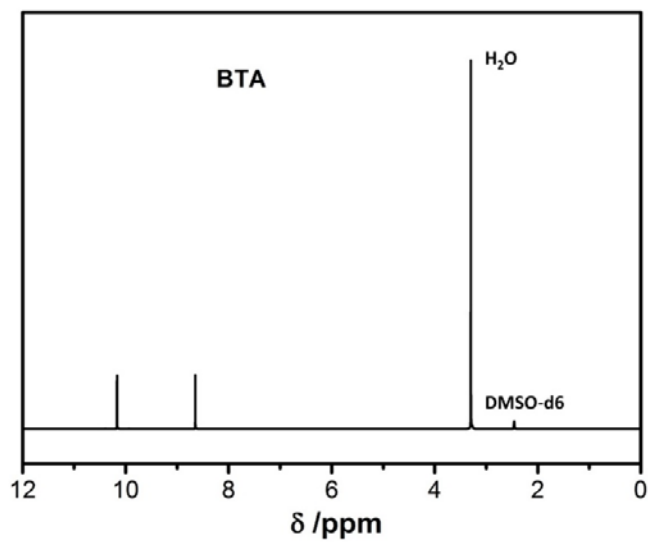


Figure S28. The ¹H-NMR spectrum of BTA in DMSO-d₆.

SUPPORTING INFORMATION

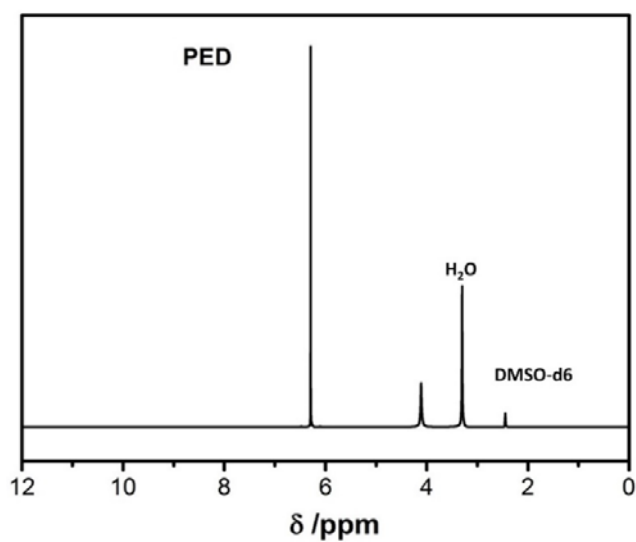


Figure S29. The ¹H-NMR spectrum of PED in DMSO-d₆.

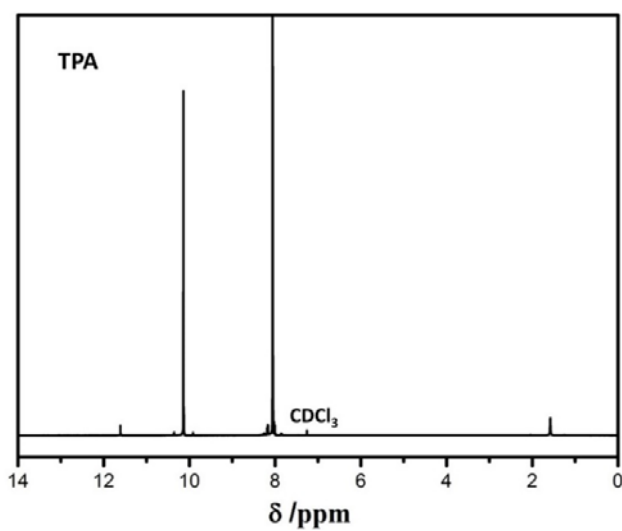


Figure S30. The ¹H-NMR spectrum of TPA in CDCl₃.

SUPPORTING INFORMATION

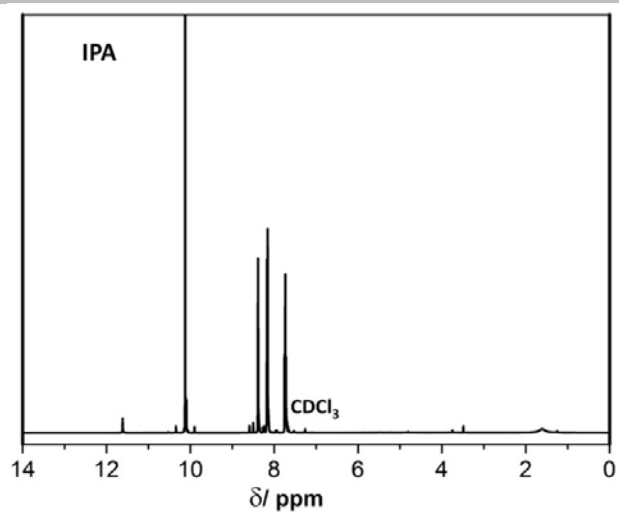


Figure S31. The $^1\text{H-NMR}$ spectrum of IPA in CDCl_3 .

SUPPORTING INFORMATION

4. Computational details for imine bond formation reaction

Density functional theory (DFT) calculations were carried out to understand the reaction mechanism between 1,2-Diaminocyclohexane and 1,3,5-Benzenetricarboxaldehyde in the presence of triazolium catalyst (the triazolium monomer was used for calculation) by using Gaussian 09 software package¹. Geometry optimization was carried out at the M062x method² with a 6-31+G(d,p) basis set³ and in implicit solvent chloroform using PCM as solvation model⁴ as implemented in Gaussian 09. The description of van der Waals interactions was improved using Grimme's empirical dispersion (GD3) correction⁵. Frequency calculations, at the same level of theory, were used to obtain thermal corrections (at 298 K) and to characterize optimized structures as transition states (only a single imaginary frequency) or intermediate (if no imaginary frequencies were found). Single point energy calculations were performed at the M06-2x/Def2-TZVP level.⁶ The Intrinsic reaction coordinate (IRC)⁷ calculations of transition states were performed to confirm the appropriate connected reactants and products.

The interaction between 1,2-Diaminocyclohexane and triazolium ring

In the experiment, the up-field shift of the C5-proton signal was observed (Figure S12) when mixing Ptriaz with 1,2-Diaminocyclohexane because of the hydrogen bonding (C5-H...N) interaction between -NH₂ and triazolium moiety, which have been also revealed by theoretical calculation, an increase of C-H from 1.079 (triazolium) to 1.097 Å (triazolium + 1,2-Diaminocyclohexane) could be observed (Figure S32). Such strong interaction between 1,2-Diaminocyclohexane and Ptriaz favorably impair the strength of the C-H bond, leading to easier ionization of the C5-proton and enhancing acidity that catalyzes the imine bond formation reaction (as evidenced by in situ ¹H NMR spectra of CC3R formation process).

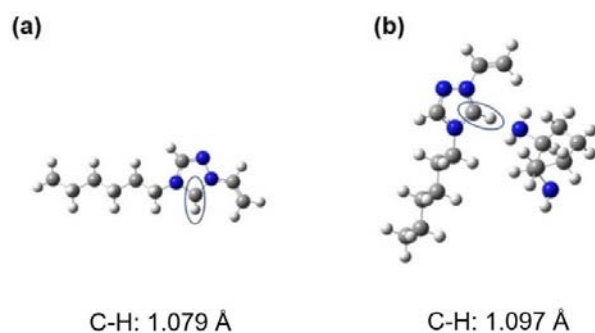


Figure S32. (a) The C5-H distance of (a) Ptriaz, (b) Ptriaz in the presence of 1,2-Diaminocyclohexane (White, H; gray, C; red, O; blue, N).

References

[1]. M. J. Frisch, G. W. Trucks, H. B. Schlegel, G. E. Scuseria, M. A. Robb, J. R. Cheeseman, G. Scalmani, V. Barone, B. Mennucci, G. A. Petersson, H. Nakatsuji, M. Caricato, X. Li, H. P. Hratchian, A. F. Izmaylov, J. Bloino, G. Zheng, J. L. Sonnenberg, M. Hada, M. Ehara, K. Toyota, R. Fukuda, J. Hasegawa, M. Ishida, T. Nakajima, Y. Honda, O. Kitao, H. Nakai, T. Vreven, J. A. Montgomery, Jr., J. E. Peralta, F. Ogliaro, M. Bearpark, J. J. Heyd, E. Brothers, K. N. Kudin, V. N. Staroverov, R. Kobayashi,

SUPPORTING INFORMATION

J. Normand, K. Raghavachari, A. Rendell, J. C. Burant, S. S. Iyengar, J. Tomasi, M. Cossi, N. Rega, J. M. Millam, M. Klene, J. E. Knox, J. B. Cross, V. Bakken, C. Adamo, J. Jaramillo, R. Gomperts, R. E. Stratmann, O. Yazyev, A. J. Austin, R. Cammi, C. Pomelli, J. W. Ochterski, R. L. Martin, K. Morokuma, V. G. Zakrzewski, G. A. Voth, P. Salvador, J. J. Dannenberg, S. Dapprich, A. D. Daniels, Ö. Farkas, J. B. Foresman, J. V. Ortiz, J. Cioslowski, and D. J. Fox, Gaussian, Inc., Wallingford CT, **2009**.

- [2]. Y. Zhao, D. G. Truhlar, *Theor.Chem. Acc.* **2008**.
- [3]. W. J. Hehre, R. Ditchfield, J. A. Pople, *J. Chem. Phys.* **1971**, *54*, 724-728.
- [4]. J. Tomasi, B. Mennucci, R. Cammi, *Cheminform* **2005**, *105*, 2999-3093.
- [5]. S. Grimme, J. Antony, S. Ehrlich, H. Krieg, *J. Chem. Phys.* **2010**, *132*, 154104-0.
- [6]. A. Schäfer, C. Huber, R. Ahlrichs, *J. Chem. Phys.* **1994**, *100*, 5829-5835.
- [7]. K. Fukui, *Acc. Chem. Res.* **1981**, *14*, 363-368.